Chemical Engineering Journal 162 (2010) 371–379

Contents lists available at ScienceDirect

Chemical Engineering Journal

journal homepage: www.elsevier.com/locate/cej

The effect of surface acidic and basic properties on the hydrogenation of aromatic rings over the supported nickel catalysts

Shenghua Hu, Mingwei Xue, Hui Chen, Jianyi Shen*

Laboratory of Mesoscopic Chemistry, School of Chemistry and Chemical Engineering, Nanjing University, Hankou Road 22, Nanjing 210093, China

ARTICLE INFO

Article history:
Received 5 January 2010
Received in revised form 29 April 2010
Accepted 12 May 2010

Keywords:
Supported nickel catalysts
Active metal surface area
Microcalorimetric adsorption
Surface acidity and basicity
Toluene hydrogenation
Phenol hydrogenation

ABSTRACT

Ni/Al_2O_3, Ni/MgAlO and Ni/MgO catalysts containing about 60 wt% of nickel were prepared by the co-precipitation method. The textural and structural properties were characterized and it was found that the dispersion of nickel was high in these catalysts. The active nickel surface area was found to be high ($78\ m^2/g_{cat.}$) in Ni/MgAlO, corresponding to the average nickel particle size of 3.5 nm. Microcalorimetric adsorption of NH_3 and CO_2 showed that the Ni/Al_2O_3 and Ni/MgO exhibited strong surface acidity and basicity, respectively, while the Ni/MgAlO possessed both surface acidity and basicity. In addition, both the initial heat and coverage were higher on Ni/Al_2O_3 than on Ni/MgO for the adsorption of toluene, indicating the strong interaction between the aromatic rings in toluene (that may act as a Lewis base due to the enriched electron densities) and the surface acidic sites on the support. The adsorption of toluene on the metallic nickel surface produced higher heat, indicating the strong interaction of the π electrons in aromatic rings of toluene with the d orbitals of surface nickel atoms. Although the adsorption of H_2 showed the higher active surface nickel area in Ni/MgAlO than in Ni/Al_2O_3, the activities of hydrogenation of toluene and phenol were significantly higher on Ni/Al_2O_3 than on Ni/MgAlO, indicating the important effect of surface acidity on the hydrogenation of aromatic rings.

1. Introduction

Supported nickel catalysts have been widely used for hydrogenation reactions of many organic compounds such as nitriles, aromatics and oils [1–12]. The properties of supports may have important impacts on the catalytic performances of supported metals. In fact, the reducibility and dispersion of supported metals depend on the interactions between the supports and supported metals. In addition, the surface acidic and basic properties may play important roles in determining the catalytic activity and selectivity.

Supports with high surface areas and appropriate preparation methods are usually required to obtain the supported nickel catalysts with high reducibility and dispersions. The techniques usually used to prepare supported nickel catalysts include impregnation [13], deposition–precipitation [12,14], sol–gel [15–17] and co-precipitation [17–19]. Supported nickel catalysts with high loadings are usually used for industrial hydrogenation processes [14,15]. It is usually difficult to obtain the supported nickel catalysts with high dispersion and loading of nickel with the conventional impregnation method. The supported nickel catalysts with high dispersion and loading may be prepared by the deposition–precipitation and sol–gel methods, but they usually involve the complicated procedures. Co-precipitation is a simple method, but there are factors such as precursors, precipitating agents, temperature and pH that affect the properties of catalysts prepared [17–19]. During the preparation of a supported metal catalyst by the co-precipitation method, the step of drying may play a key role in determining the final properties of a catalyst. The direct drying may cause severe agglomerations due to the removal of water with the high surface tension [18]. A solvent with low surface tension may be used to replace water before the drying step so that the agglomeration may be diminished [20].

The surface acidic and basic properties of a catalyst may affect the catalytic reactivity since they may affect the adsorption and desorption behavior of reactants and products. For example, the basic surface favors the selectivity to primary amines while the acidic surface promotes the formation of secondary and tertiary amines during the hydrogenation of nitriles over the supported nickel catalysts. Thus, MgO and MgAlO complex oxide prepared from hydrotalcite were used to support nickel for the hydrogenation of nitriles [1–6]. It was also found that the activity for the hydrogenation of toluene over the Ni/SiO_2–TiO_2 catalysts increased with the total number of weak and intermediate acid sites [21], whereas the hydrogenation of toluene over Pt and Pd supported on strong acidic supports (e.g. zeolite) led to the formation of by-products and carbon-deposition [22]. The activity and selectivity

* Corresponding author. Tel.: +86 25 83594305; fax: +86 25 83594305.
E-mail address: jyshen@nju.edu.cn (J. Shen).

1385-8947/$ – see front matter © 2010 Elsevier B.V. All rights reserved.
doi:10.1016/j.cej.2010.05.019

to cyclohexanone were found to be increased with the increase of surface basicity of supports for the hydrogenation of phenol over the supported palladium catalysts [23,24].

The hydrogenation of benzene to cyclohexane is an important reaction for the synthesis of nylon 6. In addition, the hydrogenation of benzene and toluene are frequently used as probe reactions to characterize metal catalysts since they are taken as the insensitive reactions with respect to the surface structures of metals [22,25,26].

Cyclohexanol and cyclohexanone may be produced by the hydrogenation of phenol, and cyclohexanol may be dehydrogenated to cyclohexanone. Cyclohexanone is an important intermediate for the production of caprolactam for nylon 6 and adipic acid for nylon 66. The selective hydrogenation of phenol for the direct formation of cyclohexanone has been studied for the supported palladium catalysts [23,24,27–46]. The hydrogenation of phenols over supported nickel catalysts was also studied as an alternative way to replace the thermal or catalytic incinerations for the treatment of wastes containing phenols [47,48].

In this work, Ni/Al_2O_3, Ni/MgAlO and Ni/MgO catalysts with the high loading of nickel (about 60 wt%) were prepared by the co-precipitation method. n-Butanol was used to replace water in the precipitates before the drying step. In this way, surface areas of the catalysts and dispersion of supported nickel were found to be significantly improved. The catalytic activities of the catalysts were evaluated by the hydrogenations of toluene and phenol, and were correlated with the number of surface metal sites and acidic/basic properties.

2. Experimental

2.1. Preparation of catalysts

The Ni/Al_2O_3, Ni/MgAlO ($MgO/Al_2O_3 = 3$, w/w) and Ni/MgO catalysts containing about 60 wt% nickels were prepared by the co-precipitation method. Specifically, desired amount of metal nitrates ($Ni(NO_3)_2{\cdot}6H_2O$, $Al(NO_3)_3{\cdot}9H_2O$ and/or $Mg(NO_3)_2{\cdot}6H_2O$, all in AR grade) were dissolved in 100 ml distilled water to form a solution (I). Desired amount of Na_2CO_3 (AR) was dissolved in 100 ml distilled water to form another solution (II). The two solutions were simultaneously dropwise added into a beaker containing 250 ml distilled water at 353 K under vigorous stirring. The precipitate formed was filtered and washed thoroughly with water until pH of the filtrate was 7. n-Butanol (about 200 ml, AR) was then added into the precipitate and heated at 353 K overnight during which water and n-butanol were evaporated. The precipitate was then dried in an oven at 393 K for 12 h.

2.2. Characterization of catalysts

The chemical compositions of the supported nickel catalysts were analyzed by an inductively coupled plasma atomic emission spectrometer (ICP-AES, Jarrell-Ash, J-A1100).

The nitrogen adsorption/desorption isotherms were determined at 77 K using a Micromeritics Gemini V 2380 autosorption analyzer. Catalysts were usually out-gassed in flowing nitrogen at 673 K for 3 h prior to the measurements, except for those dried at 393 K (the samples dried at 393 K were pretreated at 393 K). The specific surface areas were calculated using the Brunauer–Emmett–Teller (BET) method, and the pore size distributions were obtained according to the desorption branches by the Barrett–Joyner–Halenda (BJH) method.

Powder X-ray diffraction (XRD) patterns were collected on a Philips X'Pert Pro diffractometer using Ni-filtered Cu Kα radiation ($\lambda = 0.15418$ nm), operated at 40 kV and 40 mA at a scanning rate of 25°/min.

Temperature-programmed reduction (TPR) measurements were performed by using a quartz U-tube reactor loaded with about 50 mg of a dried sample in 5.03% H_2/N_2 (v/v) at a flow rate of 40 ml/min. The hydrogen consumption was monitored by a thermal conductivity detector (TCD). The reducing gas was first passed through the reference arm of the TCD before entering the reactor. The exiting gas passed through a trap filled with soda lime to remove water and possibly CO_2 and then reached the second arm of the TCD. The temperature was linearly raised from 303 to 1173 K with a rate of 10 K/min.

Microcalorimetric adsorption measurements were performed using a Tian-Calvet type C-80 microcalorimeter (Setaram, France), which was connected to a glass vacuum-dosing system, equipped with a Baratron capacitance manometer (USA) for the pressure measurement and gas handling. About 0.1 g of a catalyst was loaded, reduced for 2 h in flowing H_2 at 673 K, and then evacuated for 1 h prior to a measurement.

The adsorption of H_2 and O_2 was carried out in a home-made volumetric apparatus. The catalyst was reduced in H_2 at 673 K for 2 h and evacuated at 673 K for 1 h before the measurements. The adsorption of H_2 was performed at room temperature. After the adsorption of H_2, the sample was heated to 673 K at a rate of 10 K/min and evacuated at the temperature for 1 h. The adsorption of O_2 was performed at 673 K. The uptakes of H_2 and O_2 were obtained by extrapolating the coverage of corresponding isotherms to $P = 0$. The degree of reduction (reducibility), dispersion, active surface area and average particle size of supported nickel were calculated based on the amount of H_2 and O_2 adsorbed and loading of nickel. The surface area of metallic nickel was calculated by the uptake of H_2 assuming the molar ratio of $H/Ni_{surf} = 1$ and a surface area of 6.5 Å^2 for a Ni atom [49,50]. The amount of metallic nickel atoms in the catalyst were calculated according to the uptake of O_2 and the molar ratio of O/Ni = 1 [51]. The reduction degree was then calculated by the number of nickel atoms titrated by O_2 adsorption divided by the number of nickel atoms present in the sample. Finally, the dispersion of nickel (D) could be calculated according to the following equation: D (%) = uptake of H_2/uptake of $O_2 \times 100$, while the average Ni particle size d (nm) could be derived from the equation (d (nm) = 101/D (%)) suggested by Smith et al. assuming the spherical shape of metal particles [52].

2.3. Catalytic hydrogenations

The catalytic hydrogenation experiments were performed at atmospheric pressure in a continuous down-flow fixed-bed microreactor (a vertical glass tube with i.d. = 8 mm). 20–50 mg of a power catalyst was mixed with 2.8 g quartz sand, and placed on the glass frit of the glass reactor. The catalyst was reduced in flowing H_2 at 673 K for 2 h. An n-hexane solution containing toluene (toluene:n-hexane = 1:2, w/w) or a cyclohexane solution containing phenol (phenol:cyclohexane = 1:2, w/w) with H_2 was fed into the reactor for the hydrogenation reactions. The liquid feeds were delivered into the reactor using a 2ZB-1L10 dual-plunger infinitesimal quality metering pump. The reaction of hydrogenation of toluene was performed at 413 K with the weight hourly space velocity (WHSV) of toluene from 21 to 80 h^{-1}. The reaction of hydrogenation of phenol was operated at 423 K with the WHSV of phenol from 42 to 247 h^{-1}. The WHSV was adjusted by changing the flow rates of liquids and H_2. The products were collected using a trap in ice bath. The products were analyzed by a gas chromatograph with an FID equipped with an HP-FFAP capillary column. Turnover frequency (TOF) was calculated by dividing the number of molecules converted per second by the number of active nickel atoms on the surface measured by H_2 adsorption.

Table 1
Chemical composition, surface area and pore structure of supported nickel catalysts.

Catalyst	Chemical composition analyzed by ICP (wt%)			Treatment[a]	BET area (m^2/g)	Most probable pore sizes (nm)	Pore volume (cm^3/g)
	Ni	MgO	Al_2O_3				
Ni/Al_2O_3	62.5	–	37.5	Dried	127	3.4, 4.8	0.43
				Reduced	341	6.6	1.01
Ni/MgAlO	64.9	25.6	9.5	Dried	147	3.3, 8.0	0.59
				Reduced	244	8.9	0.87
Ni/MgO	62.7	37.3	–	Dried	125	3.5, 14.4	0.62
				Reduced	86	3.5	0.23

[a] The catalysts were dried at 393 K, followed by the reduction in H_2 at 673 K.

3. Results and discussion

3.1. Textural and structural properties of catalysts

The chemical compositions, specific surface areas and pore structural parameters of the supported nickel catalysts are summarized in Table 1. The results from ICP-AES showed that the loadings of nickel were 62.5%, 64.9% and 62.7% for the Ni/Al_2O_3, Ni/MgAlO and Ni/MgO, respectively. The weight ratio of MgO/Al_2O_3 in Ni/MgAlO was found to be about 2.7. Thus the compositions of catalysts analyzed were close to the values desired. The data in Table 1 show that the surface area and pore volume were not high for the Ni/MgO catalyst. The addition of Al_2O_3 greatly increased the surface area and pore volume of Ni/MgAlO. The Ni/Al_2O_3 possessed the highest surface area in these catalysts. Both the Ni/Al_2O_3 and Ni/MgAlO exhibited high surface areas (341 and 244 m^2/g, respectively) after the reduction at 673 K.

The XRD patterns of catalysts are shown in Fig. 1. The Ni/Al_2O_3 dried at 393 K exhibited broad and weak peaks around 24°, 36°, 44° and 63°, probably belonging to $Ni_2CO_3(OH)_2$ and $Al(OH)_3$. The broad and weak peaks observed around 23°, 35° and 61° for dried Ni/MgAlO could be assigned to $Ni_2CO_3(OH)_2$, $Al(OH)_3$ and $Mg_2CO_3(OH)_2$. No distinct XRD peaks were observed for Ni/MgO dried at 393 K. These results indicated the highly dispersed phases in the catalysts dried at 393 K.

XRD patterns for the catalysts reduced at 673 K are shown in Fig. 1(b). No distinct reflection peaks of metallic nickel were found

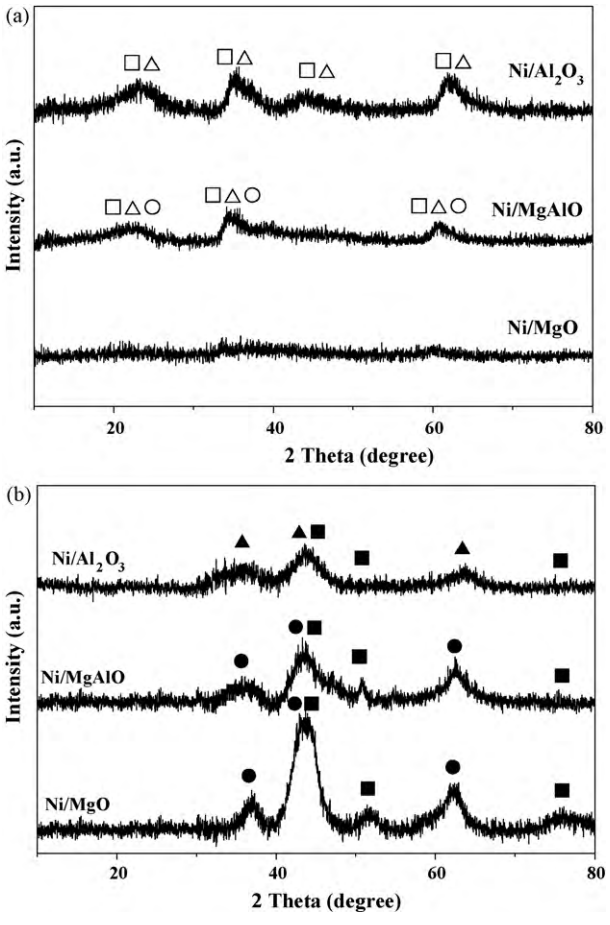

Fig. 1. XRD patterns for the supported nickel catalysts after drying at 393 K (a) and then reduction in H_2 at 673 K (b). The diffraction peaks might be assigned to phases $Ni_2CO_3(OH)_2$ (□), $Al(OH)_3$ (△), $Mg_2CO_3(OH)_2$ (○), Ni (■), Al_2O_3 (▲) and MgO (●).

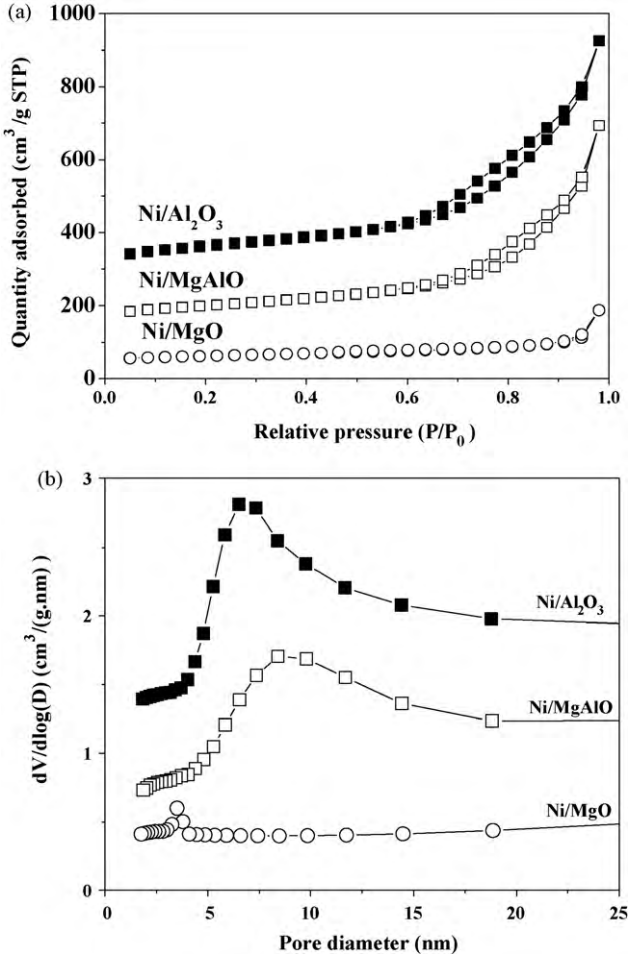

Fig. 2. N_2 adsorption–desorption isotherms (a) and pore size distributions (b) for the supported nickel catalysts reduced at 673 K.

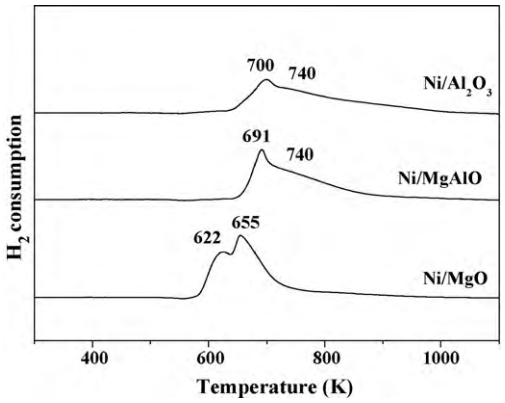

Fig. 3. TPR profiles of the supported nickel catalysts dried at 393 K.

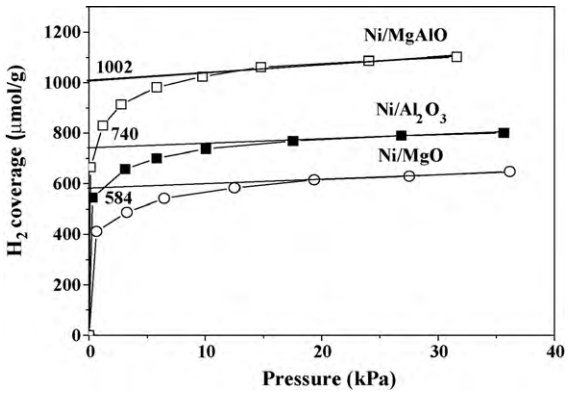

Fig. 4. Adsorption isotherms of H_2 on the supported nickel catalysts reduced at 673 K.

in the Ni/Al_2O_3, indicating the highly dispersed nickel on Al_2O_3. The three broad and weak peaks around 37°, 44° and 63° might be ascribed to γ-Al_2O_3 [19]. No nickel aluminate phases were detected in the Ni/Al_2O_3, suggesting the small crystallites of such phases in Ni/Al_2O_3. The Ni/MgO displayed five diffraction peaks around 37°, 44°, 51°, 62°, and 76°. The broad and weak peaks around 44°, 51°, and 76° were characteristic of metallic nickel, while the other peaks could be ascribed to MgO. The Ni/MgAlO also possessed broad and weak peaks around 44° and 51° for metallic nickel. The other XRD peaks for Ni/MgAlO were similar to those of MgO and Al_2O_3. Although the major peaks are overlapped for MgO and Al_2O_3 [3,53,54], they were more likely MgO since MgO was more than Al_2O_3 in Ni/MgAlO. These XRD results showed that nickel was highly dispersed in the reduced catalysts.

N_2 adsorption–desorption isotherms and pore size distributions for the supported nickel catalysts reduced at 673 K are shown in Fig. 2. The isotherms belong to type IV with H3 hysteresis loops, typical of mesopores. One peak for the pore size distribution was observed for each of these samples. The peak was weak and narrow for the Ni/MgO, while quite intensive and broad for the Ni/Al_2O_3 and Ni/MgAlO. The most probable pore diameters were found to be 3.5, 6.6 and 8.9 nm for the Ni/MgO, Ni/Al_2O_3 and Ni/MgAlO, respectively. The presence of Al_2O_3 favored the development of pores in these catalysts.

3.2. Reducibility and dispersion of supported nickel

Fig. 3 shows the TPR profiles for the three catalysts dried at 393 K. The Ni/MgO exhibited two reduction peaks around 622 and 655 K, while the Ni/Al_2O_3 showed two broad peaks around 700 and 740 K. Thus, nickel was easier reduced in Ni/MgO than in Ni/Al_2O_3, indicating the stronger interaction between NiO and Al_2O_3 than between NiO and MgO. The reduction of Ni/MgAlO was similar to that of Ni/Al_2O_3, although the Ni/MgAlO contained more MgO than Al_2O_3, indicating again the stronger interaction between NiO and Al_2O_3 than between NiO and MgO.

The adsorption of H_2 and O_2 on the reduced catalysts was carried out at room temperature and 673 K, respectively, according to which the dispersion and reducibility of supported nickel could be derived. Fig. 4 shows the H_2 adsorption isotherms and H_2 uptakes at room temperature for the catalysts reduced in H_2 at 673 K. Table 2 summarizes the information obtained by the adsorption of H_2 and O_2. According to O_2 uptakes, the degrees of reduction (reducibilities) were found to be about 43%, 74% and 89% for the Ni/Al_2O_3, Ni/MgAlO and Ni/MgO, respectively, suggesting that nickel in Ni/MgO was easier reduced than in Ni/Al_2O_3, consistent with the TPR results. The H_2 uptakes were measured to be 740, 1002 and 584 μmol/g for the Ni/Al_2O_3, Ni/MgAlO and Ni/MgO, corresponding to the active nickel areas of 57, 78 and 45 m^2/g, respectively. According to the uptakes of O_2 and H_2, the dispersions of reduced nickel were found to be about 38%, 29% and 15% for the Ni/Al_2O_3, Ni/MgAlO and Ni/MgO, respectively. The average particle sizes of reduced Ni were then calculated to be 2.7, 3.5 and 7.0 nm for the Ni/Al_2O_3, Ni/MgAlO and Ni/MgO, respectively.

Table 2
Chemisorptions of H_2 and O_2 on the supported nickel catalysts reduced at 673 K.

Catalyst	Ni/Al_2O_3	Ni/MgAlO	Ni/MgO
H_2 uptake (μmol/$g_{cat.}$)	740	1002	584
O_2 uptake (μmol/$g_{cat.}$)	1954	3497	4025
S_{Ni} ($m^2/g_{cat.}$)	57	78	45
S_{Ni} (m^2/g_{metal})	252	191	96
Reducibility (%)	42.8	74.4	88.5
Dispersion (%)	37.9	28.7	14.5
Diameter (nm)	2.7	3.5	7.0

Due to the small particles of supported nickel in these catalysts, only weak XRD peaks were observed for metallic nickel in these catalysts after reduction in H_2 at 673 K.

3.3. Surface acidic and basic properties

Microcalorimetric adsorptions of NH_3 and CO_2 were used to probe the surface acid–base properties of the reduced catalysts. Fig. 5 shows the results for the ammonia adsorption at 423 K on the catalysts reduced and evacuated at 673 K. It is seen that the initial heat and saturation coverage for the adsorption of ammo-

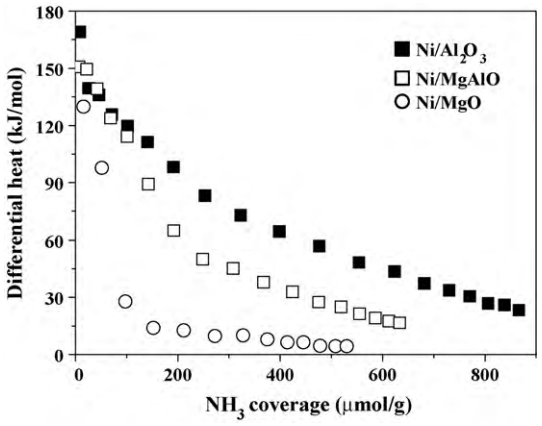

Fig. 5. Differential heat vs. coverage for NH_3 adsorption at 423 K on the supported nickel catalysts reduced and evacuated at 673 K.

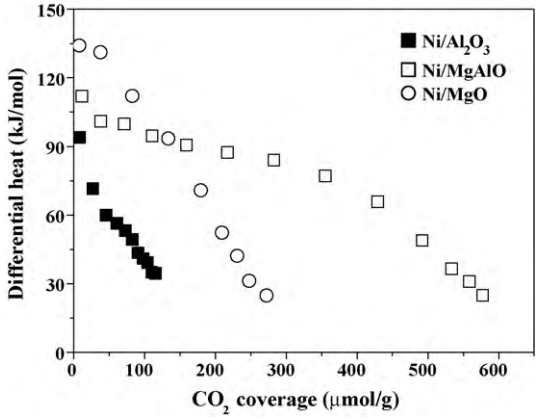

Fig. 6. Differential heat vs. coverage for CO_2 adsorption at 423 K on the supported nickel catalysts reduced and evacuated at 673 K.

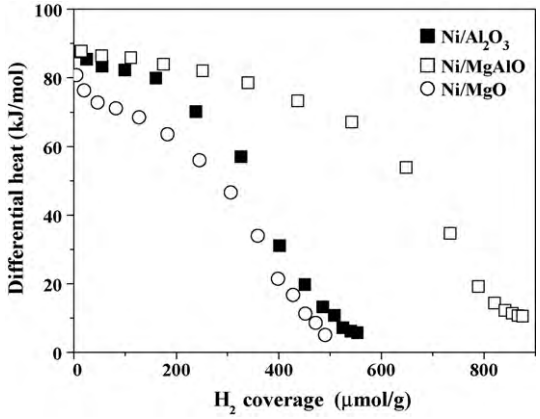

Fig. 7. Differential heat vs. coverage for H_2 adsorption at 298 K on the supported nickel catalysts reduced at 673 K.

nia were measured to be 169 kJ/mol and 870 μmol/g, respectively, for the Ni/Al_2O_3, significantly higher than the corresponding values (129 kJ/mol and 530 μmol/g) for the Ni/MgO, indicating the significantly stronger surface acidity on Ni/Al_2O_3 than on Ni/MgO. The Ni/MgAlO exhibited the initial heat of 150 kJ/mol and saturation coverage of 640 μmol/g for the adsorption of ammonia. Thus, the surface acidity on Ni/MgAlO was weaker than on Ni/Al_2O_3, but stronger than on Ni/MgO.

The heat of NH_3 adsorption was 129 kJ/mol for the Ni/MgO catalyst, but it decreased rapidly with the increase of NH_3 coverage. The initial heat might be attributed to the adsorption of NH_3 on the metallic nickel surfaces [55–57], since MgO was a basic support. The addition of 10% Al_2O_3 into Ni/MgO significantly increased the surface acidity for the Ni/MgAlO. Al_2O_3 was a typical acidic support. It is interesting to note that the reduced Ni/Al_2O_3 exhibited quite strong surface acidity, similar to that of Al_2O_3 [58], even though it contained the high loading of nickel (~60%).

The results of microcalorimetric adsorption of CO_2 at 423 K on the reduced catalysts are shown in Fig. 6. The initial heats for CO_2 adsorption on the Ni/Al_2O_3, Ni/MgAlO and Ni/MgO were 94, 112 and 134 kJ/mol, respectively. Both the initial heat and uptake for CO_2 adsorption were significantly higher on Ni/MgO than on Ni/Al_2O_3 although the surface area of Ni/MgO was much lower than that of Ni/Al_2O_3, indicating the significantly stronger surface basicity on Ni/MgO than on Ni/Al_2O_3. The addition of about 10% Al_2O_3 into Ni/MgO decreased the initial heat for CO_2 adsorption on Ni/MgAlO, but increased remarkably the uptake of CO_2 (from 270 to 560 μmol/g). Thus, the Ni/MgAlO possessed substantial amount of surface basic sites with intermediate strengths.

3.4. Microcalorimetric adsorption of H_2 and CO on supported nickel

Fig. 7 shows the results of microcalorimetric adsorption of H_2 at 298 K on the reduced catalysts. The initial heat was similar for H_2 adsorption on these catalysts (80–87 kJ/mol), consistent with the values reported in literature [1,59]. The H_2 coverage followed the same sequence for the catalysts (Ni/MgAlO > Ni/Al_2O_3 > Ni/MgO) as that titrated by the chemisorption of H_2 (see Fig. 4 and Table 2).

The results of microcalorimetric adsorption of CO at 298 K on the reduced catalysts are shown in Fig. 8. CO is usually adsorbed on metallic nickel in linear or bridged forms with different adsorption heats [60,61]. The CO/H_2 ratio of uptakes should be between 2 (for totally linear adsorption of CO) and 1 (for totally bridged adsorption of CO). The CO/H_2 ratio of uptakes was found to be about 0.8, 1.2 and 1.6 for the Ni/MgO, Ni/MgAlO and Ni/Al_2O_3, respectively. These results seemed to imply that CO was mainly bridge-adsorbed on

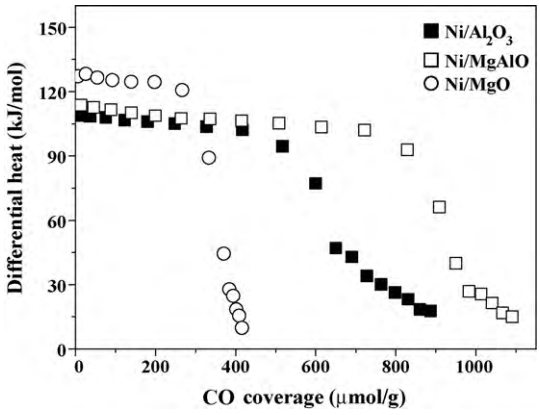

Fig. 8. Differential heat vs. coverage for CO adsorption at 298 K on the supported nickel catalysts reduced at 673 K.

Ni/MgO and Ni/MgAlO, but mostly linear-adsorbed on Ni/Al_2O_3. In addition, the heat of CO adsorption might be increased on the alkaline promoted nickel surface due to the increase of electron charges in d orbital of surface nickel [62]. The initial heat of CO adsorption was measured to be 108, 113 and 127 kJ/mol on the Ni/Al_2O_3, Ni/MgAlO and Ni/MgO, respectively. The higher initial heat for the adsorption of CO on Ni/MgO than on Ni/Al_2O_3 might be due to the different adsorbed forms of CO and/or different surface acidic/basic properties of the supports. Since MgO is a basic support, there might be some electron charges transferred from MgO to supported nickel, leading to the electron-enriched surface nickel atoms. In contrast, Al_2O_3 is an acidic support which might attract some electron charges from supported nickel, causing the electron-deficient surface nickel atoms. In fact, the above microcalorimetric adsorption of NH_3 and CO_2 showed the strong surface acidity on Ni/Al_2O_3 and strong surface basicity on Ni/MgO even after the reduction in H_2 at 673 K. The Ni/MgAlO possessed the intermediate strengths of surface acidity and basicity, and therefore the initial heat of CO adsorption on Ni/MgAlO (113 kJ/mol) was just in-between those on Ni/MgO (127 kJ/mol) and Ni/Al_2O_3 (108 kJ/mol).

3.5. Microcalorimetric adsorption of toluene on catalysts

Toluene has an electron-enriched aromatic ring and may be taken as a Lewis base. Thus, they may adsorb on acidic sites of the supports. In addition, they may adsorb on nickel atoms by donating electron charges on aromatic rings to d orbitals of surface nickel atoms. In this work, microcalorimetric adsorption of toluene was

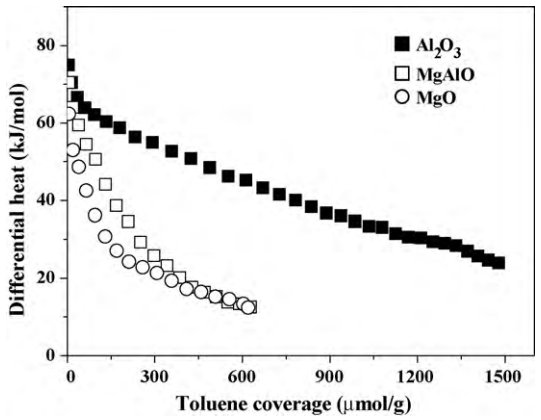

Fig. 9. Differential heat vs. coverage for toluene adsorption at 308 K on the supports treated in H_2 at 673 K.

performed for the supports and supported catalysts. Unfortunately, the microcalorimetric adsorption of phenol could not be performed since the vapor pressure of phenol was too low at room temperature.

Fig. 9 shows the results for the microcalorimetric adsorption of toluene on the supports Al_2O_3, MgAlO and MgO. Prior to the measurements, the supports were treated in H_2 at 673 K for 2 h, which were the conditions same as the reduction of catalysts. The initial heat was measured to be about 75, 70 and 62 kJ/mol for the adsorption of toluene on Al_2O_3, MgAlO and MgO, respectively. Apparently, the adsorption of toluene on acidic Al_2O_3 generated higher initial heat than that on basic MgO. Taking toluene as a Lewis base, the initial heats for the adsorption of toluene correlated well with the surface acidity of these catalysts. In addition, Al_2O_3 adsorbed much more toluene (1500 μmol/g) than MgAlO and MgO did (610 μmol/g).

Fig. 10 shows that the initial heats were about 171, 148 and 140 kJ/mol for the adsorption of toluene on the reduced Ni/Al_2O_3, Ni/MgAlO and Ni/MgO, respectively, much higher than those on the corresponding supports, indicating clearly the adsorption of toluene on the supported nickel metal surfaces. Thus, the interaction between toluene and metallic nickel was much stronger than that between toluene and the acidic sites. In addition, the acidity of supports might play a role on the adsorption of toluene on supported metallic nickel since the different initial heats were measured for the adsorption of toluene on the nickel surfaces supported on different supports. The adsorption of toluene on nickel supported on the acidic support (Al_2O_3) generated significantly higher heat than that on nickel supported on the basic support (MgO). This

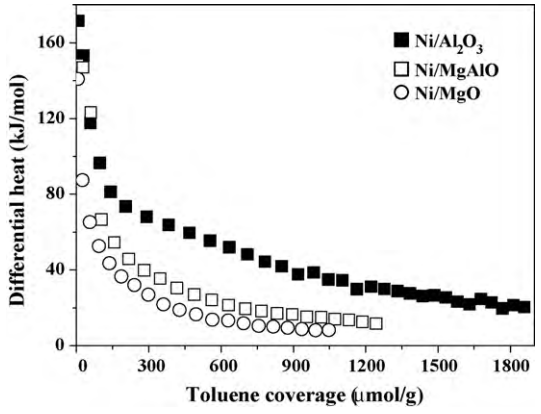

Fig. 10. Differential heat vs. coverage for toluene adsorption at 308 K on the supported nickel catalysts reduced at 673 K.

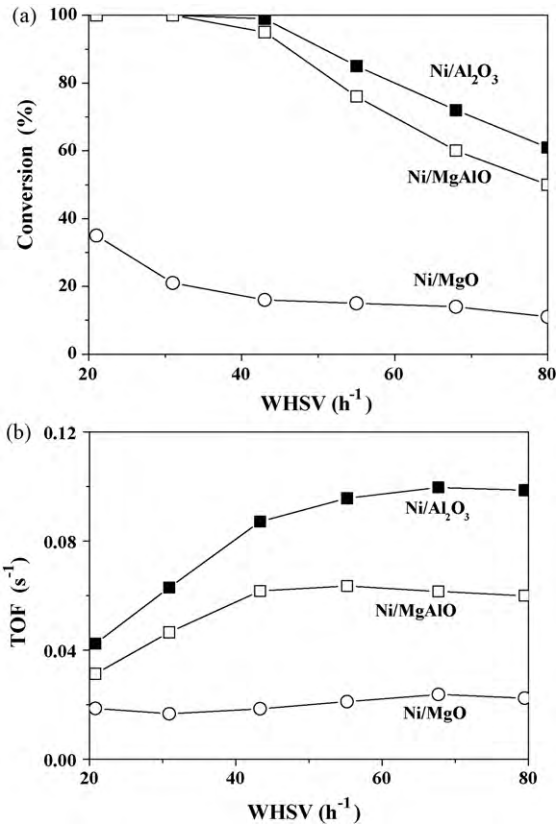

Fig. 11. Conversion (a) and TOF (b) of toluene vs. WHSV (toluene) on the supported nickel catalysts reduced at 673 K. Reaction conditions: P = 1 atm, T = 413 K and H_2/toluene = 5.

might be due to the different electron densities of supported nickel on different supports. In fact, the above result of microcalorimetric adsorption of CO showed the electron-deficient surface nickel atoms on the acidic Al_2O_3, which favored the donation of electron charges from the aromatic rings of toluene to the electron-deficient d orbitals of surface nickel atoms. In contrast, the surface nickel atoms on basic MgO might have d orbitals with enriched electron charges and thus the donation of electron charges from the aromatic rings of toluene to the d orbitals was not favored. The uptake of toluene adsorption on the reduced Ni/Al_2O_3 (1870 μmol/g), Ni/MgAlO (1280 μmol/g) and Ni/MgO (1050 μmol/g) followed the same order as their surface acidities.

3.6. Catalytic hydrogenation

Fig. 11 presents the results for the hydrogenation of toluene at 413 K over the supported nickel catalysts. Methyl cyclohexane was found to be the only product for the reaction on the catalysts. The conversion of toluene was 100% over the Ni/Al_2O_3 and Ni/MgAlO at the WHSV of toluene of 21 h^{-1}, while it was only 35% over the Ni/MgO at the same WHSV of toluene. The conversion of toluene remained 100% for the Ni/MgAlO until the WHSV of toluene was higher than 31 h^{-1}, while it was 100% for the Ni/Al_2O_3 until the WHSV of toluene was higher than 43 h^{-1}. Apparently, the activity of these catalysts for the hydrogenation of toluene followed the sequence: Ni/Al_2O_3 > Ni/MgAlO > Ni/MgO, in terms of the same mass of a catalyst loaded in the reactor.

Since the uptake of H_2 measured the number of active sites of surface nickel, the activity could be expressed in turnover frequency (TOF) as shown in Fig. 11(b). The TOF of toluene was found to increase with the increase of WHSV of toluene over the Ni/Al_2O_3

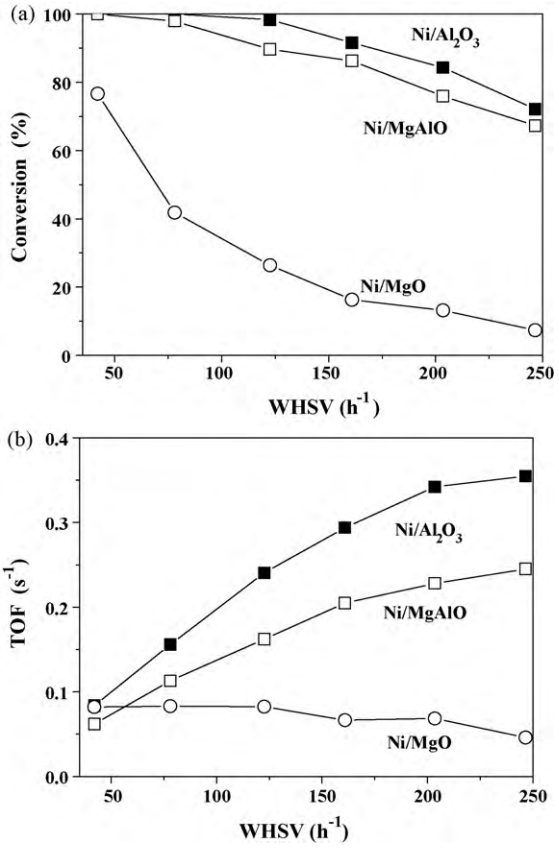

Fig. 12. Conversion (a) and TOF (b) of phenol vs. WHSV (phenol) on the supported nickel catalysts reduced at 673 K. Reaction conditions: P = 1 atm, T = 423 K and H_2/phenol = 5.

and Ni/MgAlO, and finally reached constant values for the catalysts. The maximum TOF was determined to be 0.02, 0.06 and 0.1 s^{-1} over the Ni/MgO, Ni/MgAlO and Ni/Al_2O_3, respectively, indicating again the activity sequence: Ni/Al_2O_3 > Ni/MgAlO > Ni/MgO.

The results of catalytic hydrogenation of phenol at 423 K are shown in Fig. 12. Cyclohexanol was the main product for all the catalysts, but a small amount of cyclohexanone was also formed, especially for the Ni/MgO (data were not presented). No other by-products were observed. Fig. 12(a) shows the effect of WHSV of phenol on the conversion.

The conversion of phenol was 100% over the Ni/Al_2O_3 and Ni/MgAlO at the WHSV of phenol of 42 h^{-1}, while it was only 77% over the Ni/MgO at the same WHSV of phenol. The conversion of phenol remained 100% for the Ni/MgAlO until the WHSV of phenol was higher than 78 h^{-1}, while it was 100% for the Ni/Al_2O_3 until the WHSV of phenol was higher than 125 h^{-1}. Apparently, the activity of these catalysts for the hydrogenation of phenol followed the sequence: Ni/Al_2O_3 > Ni/MgAlO > Ni/MgO, in terms of the same mass of a catalyst loaded in the reactor.

Fig. 12(b) shows the activity (TOF) of phenol hydrogenation as a function of WHSV for the catalysts. The TOF of phenol increased for the Ni/Al_2O_3 and Ni/MgAlO while it was decreased slightly for the Ni/MgO, with the increase of WHSV of phenol. At the maximum WHSV of phenol (247 h^{-1}) used in this study, the TOF of phenol was determined to be about 0.05, 0.24 and 0.35 s^{-1} on the Ni/MgO, Ni/MgAlO and Ni/Al_2O_3, respectively, indicating the same activity sequence as: Ni/Al_2O_3 > Ni/MgAlO > Ni/MgO.

The conversions of toluene and phenol versus residence time could be plotted (not shown). The conversions increased almost linearly with residence time until they approach 100% over the Ni/Al_2O_3 and Ni/MgAlO, indicating that no diffusion limitations occurred for the reactions when the conversions were lower than 100% [3]. When the conversions reached 100%, it was difficult to judge the diffusion limitations for the reactions. However, even if the conversions reached 100%, the increase of WHSV still increased the TOF (Figs. 11 and 12), indicating that more molecules could be converted over the Ni/Al_2O_3 and Ni/MgAlO until the TOF was stabilized.

Studies have shown that the activity of aromatic hydrogenation depended not only on the amounts of accessible active metal sites, but also on the surface acid–base properties [63].

In this work, the Ni/MgO with the fewest active sites of surface nickel and the weakest surface acidity, exhibited the lowest activity for the hydrogenation of toluene and phenol in the catalysts studied. The Ni/Al_2O_3 possessed fewer active sites of surface nickel, but stronger surface acidity, than the Ni/MgAlO. However, the Ni/Al_2O_3 was found to be significantly more active than the Ni/MgAlO for the hydrogenation of toluene and phenol. These facts indicated clearly that the surface acidity of supported nickel catalysts played an important role for the hydrogenation of aromatic rings, besides the number of active sites of surface nickel.

Coleman et al. [64] indicated that the Ni/Al_2O_3 and Ni/MgAlO possessed mainly the surface Lewis acidity. The surface acidity might play two roles for the hydrogenation of toluene on the supported nickel. Firstly, the surface acidity favored the adsorption of toluene since toluene can be taken as a Lewis base due to the enriched electron density on the aromatic ring with π-bonds. This has been proved by the results of microcalorimetric adsorption of toluene presented above. Secondly, the nickel atoms supported on the acidic surface might be electron-deficient due to the electron charge transfer from nickel atoms to acidic sites. The adsorption of toluene on the electron-deficient nickel atoms might be thus enhanced due to the enhanced electron donor from the aromatic rings to nickel atoms. This has also been proved by the results of microcalorimetric adsorption of CO and toluene that have discussed above.

Phenol is acidic due to its acidic hydroxyl group. Thus, phenol should be adsorbed more strongly on basic support than on acidic support. However, the activity of catalysts for the hydrogenation of phenol followed the same order as their surface acidity: Ni/Al_2O_3 > Ni/MgAlO > Ni/MgO. Thus, the adsorption of acidic hydroxyl groups on basic sites did not seem to be important for the hydrogenation of aromatic rings of phenol. Instead, the adsorption of aromatic rings on acidic sites might be important for the hydrogenation of aromatic rings of phenol. More specifically, only the aromatic rings of phenol that adsorbed on active sites of nickel might be activated and hydrogenated. In this case, the surface acidity might also play the two roles for the supported nickel for the hydrogenation of phenol to cyclohexanol, just as the roles it played for the hydrogenation of toluene to methyl cyclohexane.

4. Conclusions

(1) Ni/Al_2O_3, Ni/MgAlO and Ni/MgO catalysts containing about 60 wt% nickel were prepared by the co-precipitation method. These catalysts possessed high surface areas of active nickel due to the high loading and dispersion of supported nickel. Nickel was relatively easier to reduce in Ni/MgO than in Ni/Al_2O_3, while it was more highly dispersed in Ni/Al_2O_3 than in Ni/MgO. Thus, both the reducibility and dispersion of nickel in Ni/MgAlO were quite high, leading to the highest area of active nickel (78 $m^2/g_{cat.}$) in the three catalysts studied in this work.

(2) Microcalorimetric adsorption of NH_3 and CO_2 showed the acidic surface of Ni/Al_2O_3, but basic surface of Ni/MgO, both after the reduction. The reduced Ni/MgAlO exhibited both the surface acidity and basicity. Its surface acidity was weaker than

Ni/Al_2O_3, but stronger than Ni/MgO, while its surface basicity was weaker than Ni/MgO, but stronger than Ni/Al_2O_3.

(3) The initial heat was measured to be about 108, 113 and 127 kJ/mol for the adsorption of CO on the Ni/Al_2O_3, Ni/MgAlO and Ni/MgO, respectively, indicating that the basic support MgO might donate electron charges to, while the acidic support Al_2O_3 might withdraw electron charges from the supported nickel atoms. Thus, the surface charge density of nickel might be changed by the surface acid–base properties of supports.

(4) Both the initial heat and coverage for the adsorption of toluene were higher on the acidic Al_2O_3 than on the basic MgO, indicating the interaction between aromatic rings of toluene (as a Lewis base) and the surface acidic sites. The adsorption of toluene on the supported nickel sites generated significantly higher heat as compared to the adsorption of toluene on the supports, indicating the strong interaction between the π electrons on aromatic rings of toluene and the d orbitals of surface nickel atoms. In addition, the initial heat was higher for the adsorption of toluene on the Ni/Al_2O_3 than on the Ni/MgO, indicating the stronger interaction of aromatic rings of toluene with the electron-deficient nickel atoms on the acidic Al_2O_3, and thus probably the easier activation of aromatic rings of toluene on the electron-deficient nickel atoms.

(5) The activity of catalysts for the hydrogenation of toluene and phenol was found to follow the same order as: Ni/Al_2O_3 > Ni/MgAlO > Ni/MgO. Although the Ni/MgAlO possessed significantly more active sites of surface nickel than the Ni/Al_2O_3, the Ni/Al_2O_3 exhibited significantly higher activity than the Ni/MgAlO for the hydrogenation of toluene and phenol, indicating the important roles of surface acidity besides the number of surface nickel sites for the hydrogenation of aromatic rings. Apparently, the surface acidity favored the adsorption and activation of aromatic rings, even for the acidic phenol.

Acknowledgements

Financial supports from NSFC (20673055), MSTC (2005CB221400) and Jiangsu Province, China (BE2009145) are acknowledged.

References

[1] F.M. Cabello, D. Tichit, B. Coq, A. Vaccari, N.T. Dung, Hydrogenation of acetonitrile on nickel-based catalysts prepared from hydrotalcite-like precursors, J. Catal. 167 (1997) 142–152.
[2] F. Medina, R. Dutartre, D. Tichit, B. Coq, N.T. Dung, P. Salagre, J.E. Sueiras, Characterization and activity of hydrotalcite-type catalysts for acetonitrile hydrogenation, J. Mol. Catal. A 119 (1997) 201–212.
[3] M. Serra, P. Salagre, Y. Cesteros, F. Medina, J.E. Sueiras, Nickel and nickel-magnesia catalysts active in the hydrogenation of 1,4-butanedinitrile, J. Catal. 197 (2001) 210–219.
[4] M. Serra, P. Salagre, Y. Cesteros, F. Medina, J.E. Sueiras, Nickel-magnesia catalysts: an alternative for the hydrogenation of 1,6-hexanedinitrile, J. Catal. 209 (2002) 202–209.
[5] M. Serra, P. Salagre, Y. Cesteros, F. Medina, J.E. Sueiras, Evolution of several Ni and Ni-MgO catalysts during the hydrogenation reaction of adiponitrile, Appl. Catal. A 272 (2004) 353–362.
[6] A.C. Gluhoi, P. Mărginean, U. Stănescu, Effect of supports on the activity of nickel catalysts in acetonitrile hydrogenation, Appl. Catal. A 294 (2005) 208–214.
[7] A. Infantes-Molina, J. Mérida-Robles, P. Braos-García, E. Rodríguez-Castellón, E. Finocchio, G. Busca, P. Maireles-Torres, A. Jiménez-López, Nickel supported on porous silica as catalysts for the gas-phase hydrogenation of acetonitrile, J. Catal. 225 (2004) 479–488.
[8] P. Salagre, J.L.G. Fierro, F. Medina, J.E. Sueiras, Characterization of nickel species on several γ-alumina supported nickel samples, J. Mol. Catal. A 106 (1996) 125–134.
[9] R. Molina, G. Poncelet, Hydrogenation of benzene over alumina-supported nickel catalysts prepared from Ni(II) acetylacetonate, J. Catal. 199 (2001) 162–170.
[10] A. Jasik, R. Wojcieszak, S. Monteverdi, M. Ziolek, M.M. Bettahar, Study of nickel catalysts supported on Al_2O_3, SiO_2 or Nb_2O_5 oxides, J. Mol. Catal. A 242 (2005) 81–90.
[11] M.M. Selim, I.H.A. El-Maksoud, Spectroscopic and catalytic characterization of Ni nano-size catalyst for edible oil hydrogenation, Micropor. Mesopor. Mater. 85 (2005) 273–278.
[12] M. Gabrovska, J. Krstić, R. Edreva-Kardjieva, M. Stanković, D. Jovanović, The influence of the support on the properties of nickel catalysts for edible oil hydrogenation, Appl. Catal. A 299 (2006) 73–83.
[13] P. Braos-García, P. Maireles-Torres, E. Rodríguez-Castellón, A. Jiménez-López, Gas-phase hydrogenation of acetonitrile on zirconium-doped mesoporous silica-supported nickel catalysts, J. Mol. Catal. A 193 (2003) 185–196.
[14] M.P. González-Marcos, J.I. Gutiérrez-Ortiz, C. González-Ortiz de Elguea, J.A. Delgado, J.R. González-Velasco, Nickel on silica systems. Surface features and their relationship with support, preparation procedure and nickel content, Appl. Catal. A 162 (1997) 269–280.
[15] M.A. Ermakova, D.Y. Ermakov, High-loaded nickel-silica catalysts for hydrogenation, prepared by sol–gel route: structure and catalytic behavior, Appl. Catal. A 245 (2003) 277–288.
[16] S.R. Kirumakki, B.G. Shpeizer, G.V. Sagar, K.V.R. Chary, A. Clearfield, Hydrogenation of naphthalene over NiO/SiO_2–Al_2O_3 catalysts: structure–activity correlation, J. Catal. 242 (2006) 319–331.
[17] F. Prinetto, G. Ghiotti, P. Graffin, D. Tichit, Synthesis and characterization of sol–gel Mg/Al and Ni/Al layered double hydroxides and comparison with coprecipitated samples, Micropor. Mesopor. Mater. 39 (2000) 229–247.
[18] S. Narayanan, R. Unnikrishnan, V. Vishwanathan, Nickel-alumina prepared by constant and varying pH method: evaluation by hydrogen–oxygen chemisorption and aniline hydrogenation, Appl. Catal. A 129 (1995) 9–19.
[19] P.G. Savva, K. Goundani, J. Vakros, K. Bourikas, C. Fountzoula, D. Vattis, A. Lycourghiotis, C. Kordulis, Benzene hydrogenation over Ni/Al_2O_3 catalysts prepared by conventional and sol–gel techniques, Appl. Catal. B 79 (2008) 199–207.
[20] B. Wang, W. Zhang, W. Zhang, A.S. Mujumdar, L. Huang, Progress in drying technology for nanomaterials, Drying Technol. 23 (2005) 7–32.
[21] J.R. Grzechowiak, I. Szyszka, J. Rynkowski, D. Rajski, Preparation, characterisation and activity of nickel supported on silica-titania, Appl. Catal. A 247 (2003) 193–206.
[22] J. Chupin, N.S. Gnep, S. Lacombe, M. Guisnet, Influence of the metal and of the support on the activity and stability of bifunctional catalysts for toluene hydrogenation, Appl. Catal. A 206 (2001) 43–56.
[23] S. Scirè, C. Crisafulli, R. Maggiore, S. Minicò, S. Galvagno, Effect of the acid–base properties of Pd-Ca/Al_2O_3 catalysts on the selective hydrogenation of phenol to cyclohexanone: FT-IR and TPD characterization, Appl. Surf. Sci. 136 (1998) 311–320.
[24] S. Scirè, S. Minicò, C. Crisafulli, Selective hydrogenation of phenol to cyclohexanone over supported Pd and Pd–Ca catalysts: an investigation on the influence of different supports and Pd precursors, Appl. Catal. A 235 (2002) 21–31.
[25] F. Fajardie, J.F. Tempére, G. Djèga-Mariadassou, G. Blanchard, Benzene hydrogenation as a tool for the determination of the percentage of metal exposed on low loaded ceria supported rhodium catalysts, J. Catal. 163 (1996) 77–86.
[26] E. Rogemond, N. Essayem, R. Frety, V. Perrichon, M. Primet, F. Mathis, Characterization of model three-way catalysts. I. Determination of the accessible metallic area by cyclohexane aromatization activity measurements, J. Catal. 166 (1997) 229–235.
[27] S. Galvagno, A. Donato, G. Neri, R. Pietropaolo, Hydrogenation of phenol to cyclohexanone over Pd/MgO, J. Chem. Technol. Biotechnol. 51 (1991) 145–153.
[28] A.K. Talukdar, K.G. Bhattacharyya, S. Sivasanker, Hydrogenation of phenol over supported platinum and palladium catalysts, Appl. Catal. A 96 (1993) 229–239.
[29] N. Itoh, W.C. Xu, Selective hydrogenation of phenol to cyclohexanone using palladium-based membranes as catalysts, Appl. Catal. A 107 (1993) 83–100.
[30] G. Neri, A.M. Visco, A. Donato, C. Milone, M. Malentacchi, G. Gubitosa, Hydrogenation of phenol to cyclohexanone over palladium and alkali-doped palladium catalysts, Appl. Catal. A 110 (1994) 49–59.
[31] S.T. Srinivas, L.J. Lakshmi, P.K. Rao, Selectivity dependence on the alloying element of carbon supported Pt-alloy catalysts in the hydrogenation of phenol, Appl. Catal. A 110 (1994) 167–172.
[32] S. Narayanan, K. Krishna, Highly active hydrotalcite supported palladium catalyst for selective synthesis of cyclohexanone from phenol, Appl. Catal. A (1996) L253–L258.
[33] S. Narayanan, K. Krishna, Structure activity relationship in Pd/hydrotalcite: effect of calcination of hydrotalcite on palladium dispersion and phenol hydrogenation, Catal. Today 49 (1999) 57–63.
[34] N. Mahata, V. Vishwanathan, Gas phase hydrogenation of phenol over supported palladium catalysts, Catal. Today 49 (1999) 65–69.
[35] Y.Z. Chen, C.W. Liaw, L.I. Lee, Selective hydrogenation of phenol to cyclohexanone over palladium supported on calcined Mg/Al hydrotalcite, Appl. Catal. A 177 (1999) 1–8.
[36] N. Mahata, K.V. Raghavan, V. Vishwanathan, Influence of alkali promotion on phenol hydrogenation activity of palladium/alumina catalysts, Appl. Catal. A 182 (1999) 183–187.
[37] P. Claus, H. Berndt, C. Mohr, J. Radnik, E.J. Shin, M.A. Keane, Pd/MgO: catalyst characterization and phenol hydrogenation activity, J. Catal. 192 (2000) 88–97.
[38] S. Narayanan, K. Krishna, Hydrotalcite-supported palladium catalysts. Part II. Preparation, characterization of hydrotalcites and palladium hydrotalcites for CO chemisorption and phenol hydrogenation, Appl. Catal. A 198 (2000) 13–21.
[39] N. Mahata, V. Vishwanathan, Influence of palladium precursors on structural properties and phenol hydrogenation characteristics of supported palladium catalysts, J. Catal. 196 (2000) 262–270.
[40] N. Mahata, K.V. Raghavan, V. Vishwanathan, M.A. Keane, Influence of the charge transfer capacity of alkali and alkaline earth metals as promoters in the hydro-

genation of phenol over palladium and nickel catalysts, React. Kinet. Catal. Lett. 72 (2001) 297–302.
[41] S.G. Shore, E. Ding, C. Park, M.A. Keane, Vapor phase hydrogenation of phenol over silica supported Pd and Pd–Yb catalysts, Catal. Commun. 3 (2002) 77–84.
[42] C. Park, M.A. Keane, Catalyst support effects: gas-phase hydrogenation of phenol over palladium, J. Colloid Interface Sci. 266 (2003) 183–194.
[43] S. Velu, M.P. Kapoor, S. Inagaki, K. Suzuki, Vapor phase hydrogenation of phenol over palladium supported on mesoporous CeO_2 and ZrO_2, Appl. Catal. A 245 (2003) 317–331.
[44] U.R. Pillai, E. Sahle-Demessie, Strontium as an efficient promoter for supported palladium hydrogenation catalysts, Appl. Catal. A. 281 (2005) 31–38.
[45] L.M. Sikhwivhilu, N.J. Coville, D. Naresh, K.V.R. Chary, V. Vishwanathan, Nanotubular titanate supported palladium catalysts: the influence of structure and morphology on phenol hydrogenation activity, Appl. Catal. A 324 (2007) 52–61.
[46] K.V.R. Chary, D. Naresh, V. Vishwanathan, M. Sadakane, W. Ueda, Vapour phase hydrogenation of phenol over Pd/C catalysts: a relationship between dispersion, metal area and hydrogenation activity, Catal. Commun. 8 (2007) 471–477.
[47] E.J. Shin, M.A. Keane, Catalytic hydrogen treatment of aromatic alcohols, J. Catal. 173 (1998) 450–459.
[48] E.J. Shin, M.A. Keane, Gas-phase hydrogenation/hydrogenolysis of phenol over supported nickel catalysts, Ind. Eng. Chem. Res. 39 (2000) 883–892.
[49] C.H. Bartholomew, R.J. Farrauto, Chemistry of nickel-alumina catalysts, J. Catal. 45 (1976) 41–53.
[50] D.G. Mustard, C.H. Bartholomew, Determination of metal crystallite size and morphology in supported nickel catalysts, J. Catal. 67 (1981) 186–206.
[51] R.B. Pannell, K.S. Chung, C.H. Bartholomew, The stoichiometry and poisoning by sulfur of hydrogen, oxygen and carbon monoxide chemisorption on unsupported nickel, J. Catal. 46 (1977) 340–347.
[52] J.S. Smith, P.A. Thrower, M.A. Vannice, Characterization of Ni/TiO_2 catalysts by TEM, X-ray diffraction, and chemisorption techniques, J. Catal. 68 (1981) 270–285.
[53] E. Kiš, R. Marinković-Nedučin, G. Lomić, G. Bošković, D.Ž. Obadović, J. Kiurski, P. Putanov, Structural and textural properties of the $NiO–Al_2O_3$ catalyst, Polyhedron 17 (1998) 27–34.
[54] B. Vos, E. Poels, A. Bliek, Impact of calcination conditions on the structure of alumina-supported nickel particles, J. Catal. 198 (2001) 77–88.
[55] M.J.F.M. Verhaak, A.J. van Dillen, J.W. Geus, Measuring the acid–base properties of supported nickel catalysts using temperature-programmed desorption of ammonia, Appl. Catal. A 105 (1993) 251–269.
[56] A. Borgna, R. Fréty, M. Primet, M. Guénin, Modifications of surface properties of nickel/silica catalysts by nitrogen-containing compounds. Part I. Ammonia, Appl. Catal. 76 (1991) 233–254.
[57] A. Chattopadhyay, H. Yang, J.L. Whitten, Adsorption of ammonia on Ni(1 1 1), J. Phys. Chem. 94 (1990) 6379–6383.
[58] J. Shen, R.D. Cortright, Y. Chen, J.A. Dumesic, Microcalorimetric and infrared spectroscopic studies of γ-$A1_2O_3$ modified by basic metal oxides, J. Phys. Chem. 98 (1994) 8067–8073.
[59] J. Shen, B.E. Spiewak, J.A. Dumesic, Microcalorimetric studies of CO and H_2 adsorption on nickel, nickel-boride, and nickel-phosphide catalysts, Langmuir 13 (1997) 2735–2739.
[60] M. Cerro-Alarcón, B. Bachiller-Baeza, A. Guerrero-Ruiz, I. Rodríguez-Ramos, Effect of the reduction-preparation method on the surface states and catalytic properties of supported-nickel particles, J. Mol. Catal. A 258 (2006) 221–230.
[61] J. Álvarez-Rodríguez, M. Cerro-Alarcón, A. Guerrero-Ruiz, I. Rodríguez-Ramos, A. Arcoya, Effect of nickel precursor and the copper addition on the surface properties of Ni/KL-supported catalysts for selective hydrogenation of citral, Appl. Catal. A 348 (2008) 241–250.
[62] B.E. Spiewak, J. Shen, J.A. Dumesic, Microcalorimetric studies of CO and H_2 adsorption on nickel powders promoted with potassium and cesium, J. Phys. Chem. 99 (1995) 17640–17644.
[63] S.D. Lin, M.A. Vannice, Hydrogenation of aromatic hydrocarbons over supported Pt catalysts. III. Reaction models for metal surfaces and acidic sites on oxide supports, J. Catal. 143 (1993) 563–572.
[64] L.J.I. Coleman, W. Epling, R.R. Hudgins, E. Croiset, Ni/Mg–Al mixed oxide catalyst for the steam reforming of ethanol, Appl. Catal. A 363 (2009) 52–63.